Journal of the Research Institute of Basic Sciences,
Korea Maritime University, Vol. 3, 1993.

Evaluation of Compressive Strength of Unidirectionally Carbon–Fiber Reinforced Composite Material

Yun Hae Kim

Department of Material Engineering
Korea Maritime University, Pusan, Korea

Abstract

Compression tests for a unidirectional CFRP were carried out for a wide range of specimen lengths, three different configurations of end tab edges and two different end tab materials under the conditions of constant specimen thickness. The relation of $\sigma_c - L$ is to be classified into two parts, namely, a part where the compressive strength σ_c is nearly constant independent of specimen length L and a part where σ_c decreases with increasing L. The apparent compressive strength measured by Celanese test method was lower than the true compressive strength because of the stress concentration near the end tab edges of the specimen. The true compressive strength was was obtained by using the specimen where the specimen lengths of 3.2mm and 6.4mm and the material of end tab is stainless steel.

Introduction

High performance composites are being applied to engineering applications because of their case of fabrication, light weight, and economy [1]. There are various compression test methods for unidirectional composite materials [2, 3] but they use the different specimen length without discussing the effect of specimen length in detail. On the other hand, it is found that the

compressive strengths of unidirectional composites measured by these test methods vary significantly and most of these test methods are not approved as standards at present except ASTM Standard D 3410. Many studies on the compressive strength of unidirectionally reinforced composite materials have been made [4–11]. S. C. Tan [6] pointed out that the Celanese test method should not be recommended for measuring the compressive strength of unidirectional graphite/epoxy composites because the apparent strength of a unidirectional graphite/epoxy laminate measured by the Celanese specimen is much lower than the true compressive strength. N. R. Adsit [5] showed that the compression test method for rigid plastic (Boeing–Modified ASTM D 695) is not adequate for high modulus composite materials. H. T. Hahn and J. G. Williams [7] examined compression failure mechanisms in unidirectional composites, and showed that for stiff resins failure was characterized by the formation of a kink band but for soft resins shear crippling was in the form of buckling of fibers on a microscopic scale.

From the above discussion, we can find that we are in need of an adequate compression test method in order to evaluate the compressive strength exactly.

In this paper, the effects of specimen length and stress concentration on the compressive strength of unidirectionally carton–fiber reinforced plastic were investigated.

Materials and experimental procedure

The materials fabricated from either PAN-based (a fiber content of 63 percent, 130°C hardened type) or pitchbased (a fiber content of 53 percent, 130°C hardened type) unidirectional prepreg were used. The end tab plates were bonded onto the CFRP plates using the room temperature curing adhesive. The specimens were cut out by a diamond–tipped saw from these plates. To measure elastic modulus, the test pieces were instrumented with

strain gage on both sides of the gage section. Compression tests for the unidirectional CFRP were carried out for a wide range of specimen lengths, three different configurations of end tab edges and two different end tab materials under the conditions of constant specimen thickness. The debonding process of stainless tab was confirmed by using moire grid sheet. All tests were performed by using the Celanese method (conical shaped wedge fixture) at room temperature. The specimen configurations and a compression test fixture are shown in Figs. 1 and 2. Figure 3 shows a photograph of compression test fixture.

Experimental results and discussion

Figure 4 shows typical compressive stress–strain curves obtained from the compression tests. The type such as Fig. 4(a) was observed in the test pieces that failed by stress concentration at the end tab edges without macrobuckling. The type such as Fig. 4(b) was observed in the failure accompanied by debonding of end tab edges. In case of Fig. 4(b), the divergence of the strain gage signals on opposite sides of the gage section means the delamination of the end tab edges.

Figure 5 shows the relation between compressive strength σ_c and specimen length L. The solid lines mean the results obtained from the compression test of PAN–based CFRP and the broken lines mean that of pitch–based CFRP. The relation of $\sigma_c - L$ is to be classified into two parts, namely, a part where σ_c is nearly constant independent of L and a part where σ_c decreases with increasing L. It can be considered that the decrease of the compressive strength in the $\sigma_c - L$ relation is due to the complicated effects of elastic buckling etc. It is concluded that within the limits of our experimental results the compressive strength is nearly constant if the specimen lengths are in the range between 3.2mm and 12.7mm. This fact also means that in the part of the constant σ_c the stress concentrations at end tab edges control σ_c.

It is evident from these data that the apparent compressive strength measured by ASTM Standard D 3410 (L=12.7 mm) is lower than the true compressive strength because of the stress concentrations near the end tab edges. This result is well coincided with that of references [6].

The failure models for each type of the specimen are shown in Fig. 6. As shown in these figures, in the case of type B specimen the true compressive strength was not obtained because of the stress concentrations near the end tab edges of the specimen. To reduce the stress concentrations at end tab edges, the specimen with curvature in end tab edges (R25) which has slight stress concentrations at the end tab edges was used. As the result of the improvement, the fracture due to the stress concentrations at the end tab edges was prevented and the compressive strength became much higher than that of type B specimen. Nevertheless, the true compressive strength was not obtained. This is due to the stress concentrations after delamination. In the case of $L = 25.4$mm, the compressive strengths of type B specimens are reversely lower than those of type B specimens, as shown in Fig. 5. This is perhaps due to the fact that the equivalent specimen length is longer than 25.4mm because the end tab of type C specimen was machined to the specimen with curvature in end tab edges.

On the other hand, the type A specimen where the material of the end tab is stainless steel and the specimen lengths are 3.2mm and 6.4mm showed the highest values in compressive strength, as shown in Fig. 5. It can be considered that the highest values in compressive strength are resulted from the sheath effect of the stainless tab due to the development of delamination of the end tab edges. Figure 7 shows debonding process of the stainless tab. It is clear that the adhesive layer between the end tab and CFRP is debonded and then the stainless tab plays an important role in compressive strength of unidirectional CFRP. We call this the sheath effect of the stainless tab. Consequently, the stress concentrations are relieved in end tab edges and then the highest values are obtained owing to the sheath effect of the

stainless tab. This value nearly coincided with the true value. However, the compressive strength obtained from the type A specimen where the specimen length was 12.7mm, was rather lower than that of type B specimen because of complicated effects such as elastic buckling etc. due to the development of delamination at end tab edges. Figure 8 shows the fracture pattern of type A specimen.

Conclusions

The effects of specimen length and stress concentration on the compressive strength of unidirectional CFRP were investigated. Compression tests for unidirectional CFRP were carried out for a wide range of specimen lengths, three different configurations of end tab edges, and two different end tab materials under the condition of constant specimen thickness. The results obtained can be summarized as follows:

1. The apparent compressive strengths of unidirectional CFRPs measured by the Celanese compression test method (L=12.7mm) are lower than the true compressive strength because of the stress concentrations near the end tab edges. The true compressive strength is obtained by using the type A specimen where the end tab material is stainless steel and the specimen lengths are 3.2mm and 6.4mm.

2. Within the limits of our experimental results, the apparent compressive strength is GFRP tab specimen is nearly constant if the specimen lengths are in the range between 3.2mm and 12.7mm, and is about 65 percent of the true strength. This fact means that in the region of constant σ_c the stress concentrations at end tab edges control σ_c. To reduce the stress concentrations at the end tab edges, the type C specimen with curvature in end tab edges which has slight stress concentration at the end tab edge was used. In spite of the improvement the apparent compressive strength was not increased so much.

References

1. L. J. Broutman and R. H. Krock (edited), Composite Materials, Vol. 3, Engineering Applications of Composites, Academic Press, 1974.
2. "Compressive Properties of Unidirectional or Crossply Fiber–Resin Composites", ASTM Standard D 3410–87, Amer. Soc. Test. and Mater., Philadelphia, 1975.
3. "SACMA Recommended Test Method for Compressive Properties of Oriented Fiber–Resin Composites", Recommended Method SRM 1–88, Suppliers of Advanced Composite Materials Association, Washington DC, 1989.
4. D. Hull, An Introduction to Composite Material, Cambridge University Press, 1981.
5. N. R. Adsit, "Compression Testing of Graphite/Epoxy", Compression Testing of Homogeneous Materials and Composites, ASTM STP 808, R. Chait an R. Papirno, Eds., Amer. Soc. Test. and Mater., 175–186, 1983.
6. S. C. Tan, "Stress analysis and the Evaluation of Celanese and IITRI Compression Test Specimens", Proc. Amer. Soc. for Composites (5th Technical Conference), 827–838, 1990.
7. H. T. Hahn and J. G. Williams, "Compression Failure Mechanisms in Unidirectional Composites", Composite Materials : Testing and Design (Seventh Conference), ASTM STP 893, J. M. Whitney Ed., Amer Soc. Test. Mater., Philadelphia, 115–139, 1986.
8. N. L. Hancox, "The Compression Strength of unidirectional Carbon Fiber Reinforced plastic", J. Mater. Sci., 10, 234–242, 1975.
9. C. R. Chaplin, "Compressive Fracture in Unidirectional Glass–Reinforced Plastics", J. Mater. Sci., 12, 347–352, 1977.

10.] D. F. Adams and E. M. Odom, "Influence of Test Fixture Configuration on the Measured Compressive Strength of a Composite Material", J. Compo. Tech. and Res., 13(1), 1991.

11. J. Haeberle and F. L. Matthews, "Studies on Compressive Failure in Unidirectional CFRP Using an Improved Test Method", 4th Euro. Conf. Compos. Mater., Stuttgart, 517–523, 1990.

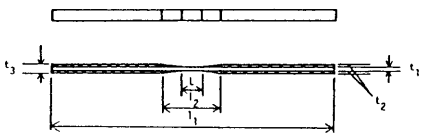

(a) Type A specimen (Stainless tab)
L=6.4, 12.7 l_1=140 l_2=19, 26
t_1=2 t_2=1 t_3=4

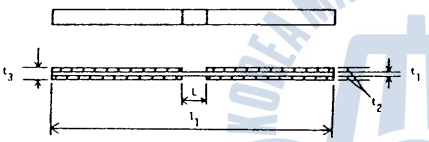

(b) Type B specimen (GFRP tab)
L=3.2, 6.4, 12.7, 25.4 l_1=140, 150
t_1=2 t_2=2 t_3=6

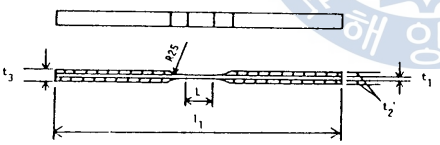

(c) Type C specimen (GFRP tab)
L=3.2, 6.4, 8, 12.7, 25.4 l_1=140, 150
t_1=2 t_2=2 t_3=6

Fig.1 Specimen configurations (Dimension : mm)

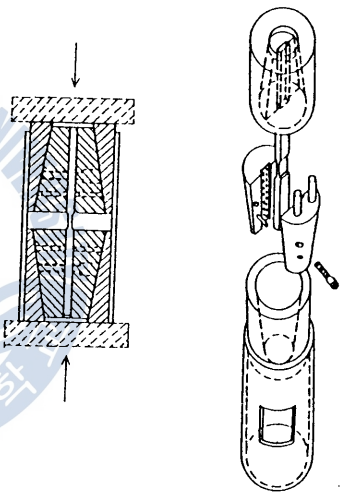

Fig.2 Compression test fixture
(ASTM Standard D 3410 test method)

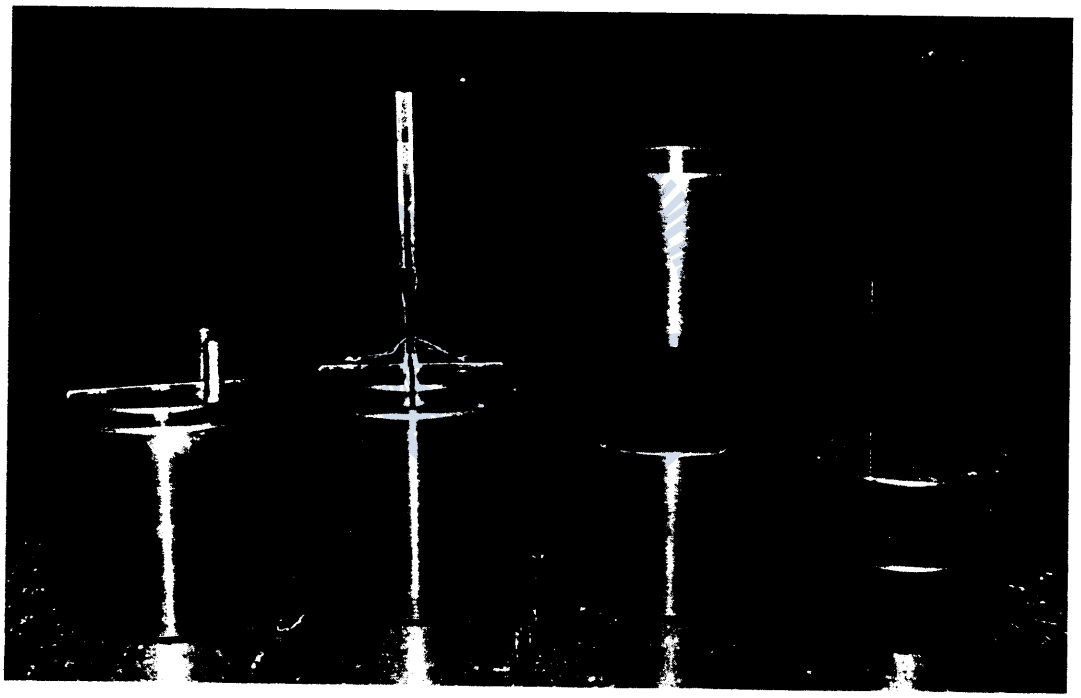

Fig.3 A photograph of compression test fixture

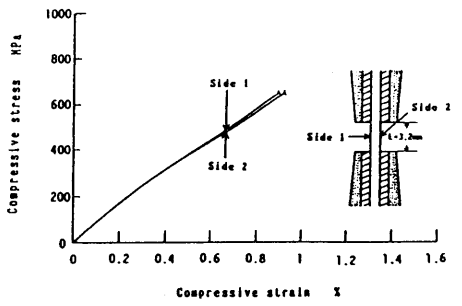

(a)

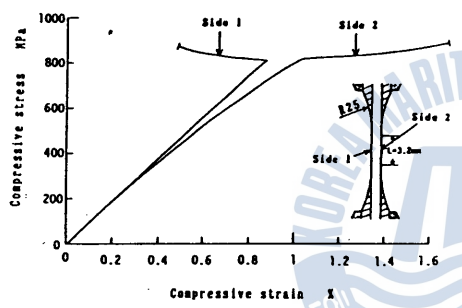

(b)

Fig.4 Typical compressive stress-strain curves

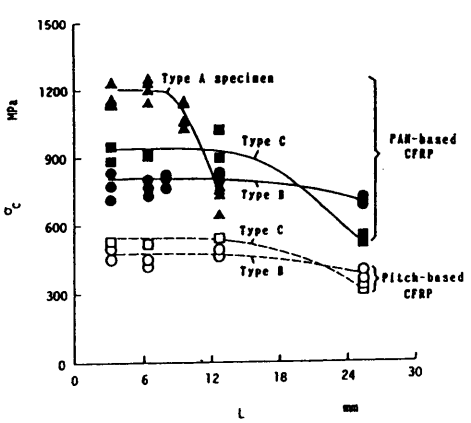

Fig.5 Relationship between compressive strength σ_c and specimen length L (See the symbols of Fig.6)

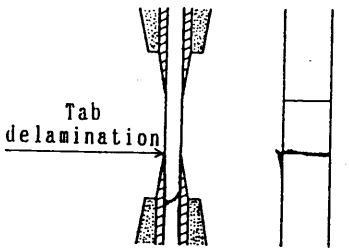

L: Small

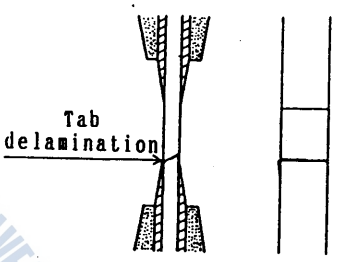

L:Large

(a) Type A specimen (stainless tab)

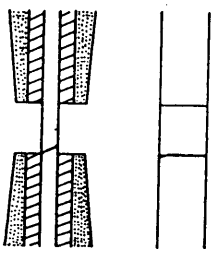

(b) Type B specimen (GFRP tab)

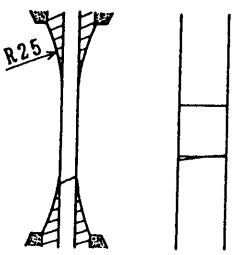

(c) Type C specimen (GFRP tab)

Fig.6 Fracture modes

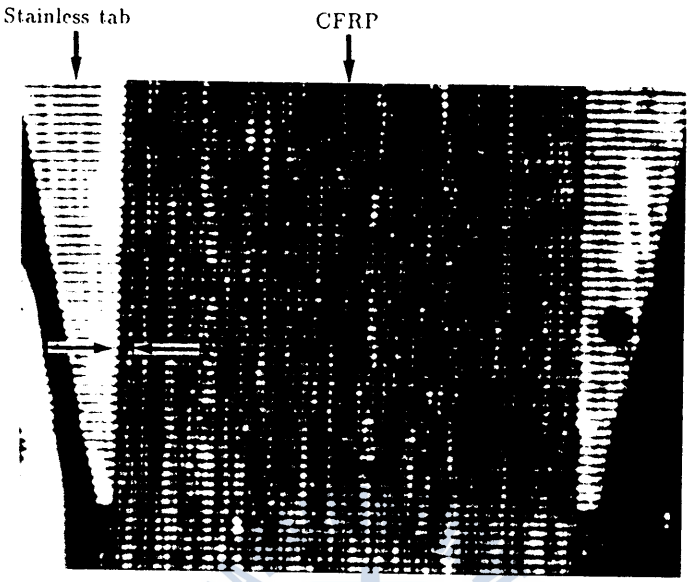

$$\frac{\sigma_c}{\sigma_{c,f}} = 0\%$$

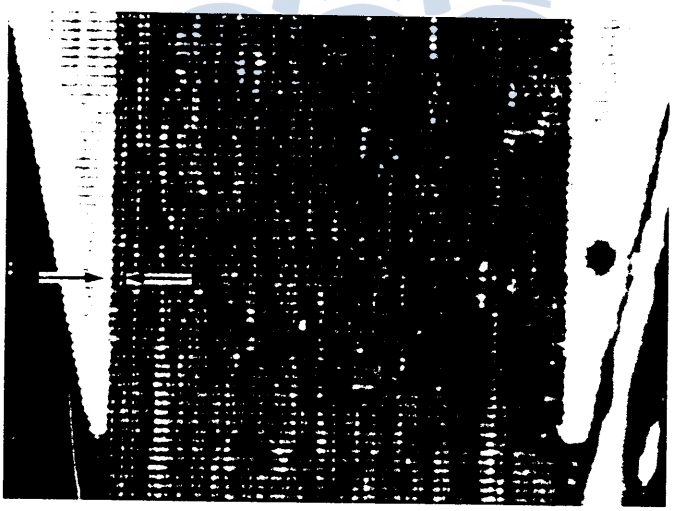

$$\frac{\sigma_c}{\sigma_{c,f}} = 6\%$$

σ_c : Compressive stress

$\sigma_{c,f}$: Compressive fracture stress

$\sigma_{c,f}$ = 1240 MPa

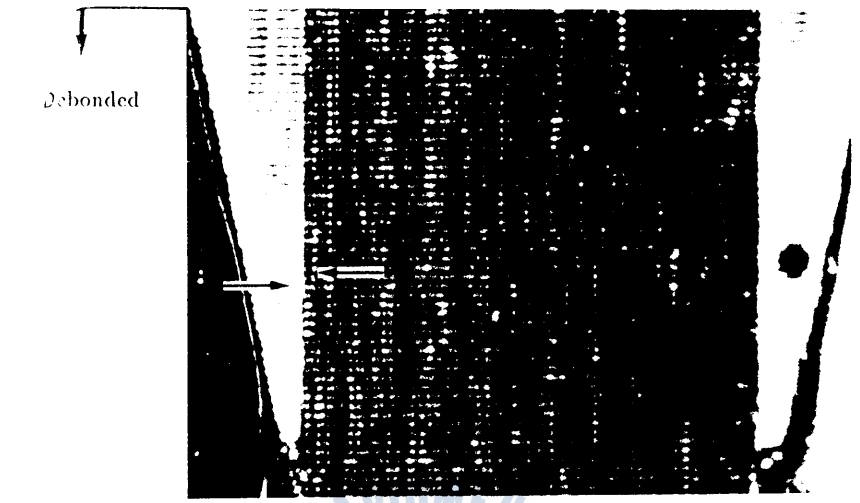

$$\frac{\sigma_c}{\sigma_{c,f}} = 49\%$$

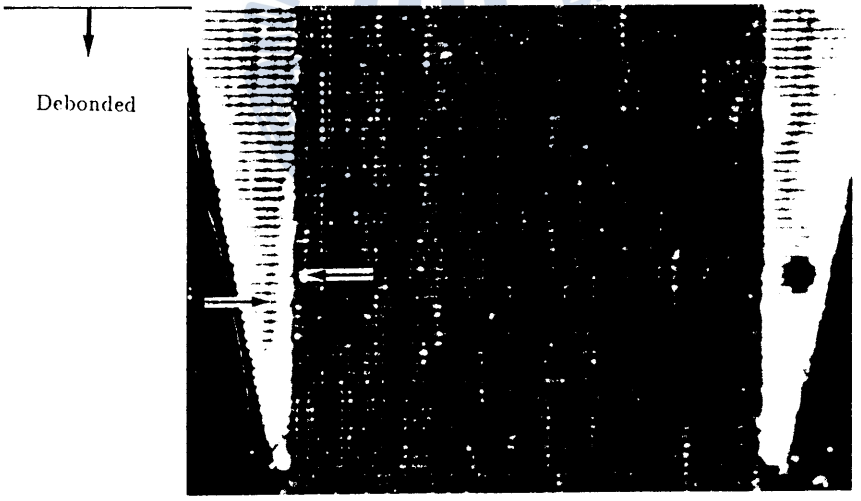

$$\frac{\sigma_c}{\sigma_{c,f}} = 73\%$$

σ_c : Compressive stress
$\sigma_{c,f}$: Compressive fracture stress

$\sigma_{c,f}$ = 1240 MPa

The process of sheath effect of the stainless tab

Table 1. Computational Results

	Problem Size n × m											
	7×1		7×5		10×1		10×5		15×1		15×5	
	W_j		W_j		W_j		W_j		W_j		W_j	
	1.5 - 2.5	2.5 - 3.5	1.5 - 2.5	2.5 - 3.5	1.5 - 2.5	2.5 - 3.5	1.5 - 2.5	2.5 - 3.5	1.5 - 2.5	2.5 - 3.5	1.5 - 2.5	2.5 - 3.5
Shi	A 0.01229 M 0.03718 O 3/10 T 0.10	A 0.00194 M 0.00542 O 0/10 T 0.13	A 0.02269 M 0.12476 O 2/10 T 0.14	A 0.00369 M 0.01495 O 0/10 T 0.21	A 0.05786 M 0.17357 O 0/10 T 0.59	A 0.00723 M 0.02621 O 0/10 T 0.97	A 0.01722 M 0.04065 O 1/10 T 0.44	A 0.00404 M 0.01092 O 0/10 T 0.66	A 0.09852 M 0.20495 O 0/10 T 1.95	A 0.02070 M 0.05475 O 0/10 T 3.12	A 0.07150 M 0.15827 O 1/10 T 0.72	A 0.01227 M 0.02365 O 0/10 T 1.20
Kohda/ Inoue	A 0.00312 M 0.02686 O 4/10 T 0.37	A 0.00007 M 0.00053 O 7/10 T 0.67	A 0.00317 M 0.01977 O 7/10 T 0.33	A 0.00033 M 0.00207 O 7/10 T 0.77	A 0.00024 M 0.00212 O 8/10 T 5.20	A 0.00003 M 0.00027 O 6/10 T 9.17	A 0.00282 M 0.01527 O 7/10 T 2.83	A 0.00015 M 0.00085 O 8/10 T 6.35	A 0.00038 M 0.00382 O 9/10 T 20.53	A 0.00001 M 0.00011 O 9/10 T 35.61	A 0.00148 M 0.01316 O 7/10 T 9.26	A 0.00016 M 0.00091 O 8/10 T 20.72
Proposed Method	A 0.00026 M 0.00138 O 6/10 T 0.62	A 0.00001 M 0.00010 O 9/10 T 0.94	A 0.00087 M 0.00871 O 9/10 T 0.52	A 0.00024 M 0.00217 O 8/10 T 0.86	A 0.0 M 0.0 O 10/10 T 9.40	A 0.0 M 0.0 O 10/10 T 13.93	A 0.00039 M 0.00386 O 9/10 T 4.73	A 0.0 M 0.00003 O 9/10 T 9.02	A 0.0 M 0.0 O 10/10 T 29.18	A 0.0 M 0.0 O 10/10 T 42.57	A 0.00085 M 0.00855 O 9/10 T 13.90	A 0.0 M 0.0 O 10/10 T 25.06
Simulated Annealing	A 0.00337 M 0.02786 O 6/10 T 49.59	A 0.00192 M 0.00515 O 2/10 T 42.63	A 0.00285 M 0.01977 O 8/10 T 63.96	A 0.00102 M 0.00390 O 4/10 T 45.57	A 0.01321 M 0.03255 O 2/10 T 154.28	A 0.02542 M 0.04472 O 0/10 T 167.03	A 0.00255 M 0.01527 O 6/10 T 133.28	A 0.00786 M 0.01682 O 0/10 T 88.28	A 0.02401 M 0.05579 O 3/10 T 365.53	A 0.05056 M 0.06631 O 0/10 T 410.63	A 0.00102 M 0.00855 O 8/10 T 366.63	A 0.01424 M 0.02301 O 0/10 T 189.39

A: Average relative error of 10 test problems
M: Maximum relative error of 10 test problems
O: Optimality rate
T: Average execution time of 10 test problems (sec)

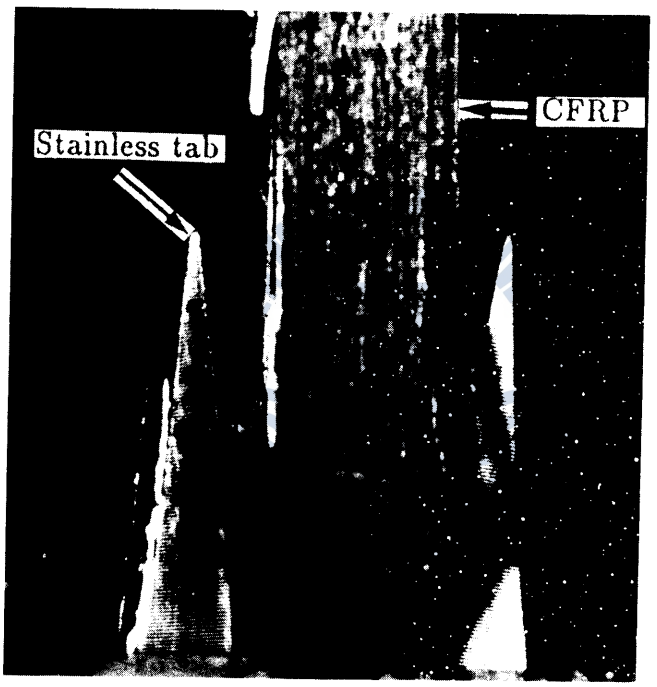

Fig. 8 Fracture pattern